

latter result by assuming a reasonable pairing interaction strength admixing seniority-one states and considering seniority-three states as perturbations. In their survey work they varied parameters smoothly and did not consider the details of the actual single particle states, so that their result is equally applicable to the excited state in Pt¹⁹⁵. Arima and Horie²² were also able to account for the value of $\mu(\text{Hg}^{201})$ by configuration mixing, but their oscillator potential is unrealistically deep. Finally, one may consider a particle-core coupling model²³ which could account for the $\frac{3}{2}^-$, $\frac{5}{2}^-$ doublet at

²² Akito Arima and Hisashi Horie, *Progr. Theoret. Phys. (Kyoto)* **11**, 509 (1954).

²³ A. Gal, *Phys. Letters* **20**, 414 (1966).

99 and 129 keV. In the simplest model the core would be the first 2+ state of Pt¹⁹⁴; and one obtains, using its moment (see above) together with that of the ground state of Pt¹⁹⁵, the prediction of $\mu(\frac{3}{2}) \simeq +0.10$, which is far from the measured value. This lack of agreement is not, however, a fair test of the particle-core coupling picture since there is another close-lying $\frac{3}{2}$, $\frac{5}{2}$ doublet at 210 and 240 keV, and none of the states involved is expected to be particularly pure.

ACKNOWLEDGMENT

We would like to thank Professor Robert Ogilvie for carrying out the electron-beam analysis of the alloys.

Range-Energy Relation and Energy Loss of Fission Fragments in Solids*

S. KAHN AND V. FORGUE

Aerojet-General Nucleonics, San Ramon, California

(Received 12 April 1967)

The energies of fission fragments transmitted through Al, Ni, Ag, Au, and U-Pd have been measured with surface-barrier detectors. The results, converted to the Lindhard-Scharff-Schiott (LSS) dimensionless parameters $k\rho$ (range) and ϵ (energy), were found to fit the empirical equation

$$k\rho = 1.158\epsilon^{1/2}[1 - \exp(0.0987\epsilon)] + 0.01939\epsilon$$

in the region $12 \leq \epsilon \leq 348$. These results are 10–20% lower than those predicted by the LSS theory. A description is given of the effect of relatively simple modifications to this theory, and suggestions are presented for a more rigorous theoretical approach.

I. INTRODUCTION

A KNOWLEDGE of the range of fission fragments and their energy loss in solid and gaseous media is important to practical applications of fission chemistry and to direct energy conversion via the fission electric cell. Such knowledge is also directly applicable to radiation-induced ionization for space-charge neutralization in thermionics and to nonthermal ionization in magnetohydrodynamics.

Neither the Bohr theory¹ nor the Lindhard-Scharff-Schiott (LSS)² theory fits the available data; furthermore, empirical equations derived from different sets of experimental data cannot be compared. One of the complications in trying to unify the available data is the obvious difference between the slowing-down mechanisms in solids and gases; i.e., the density effect associated with gases at low pressures.³ While we have

performed differential energy-loss experiments in both media, this paper gives the results only for the solid absorbers; the gaseous absorber work will be reported at a later date.

We have derived an empirical range-energy expression from our data for fission fragments in Al, Ni, Ag, Au, and U-Pd absorbers that gives fair agreement ($\pm 5\%$) with other experimental results for heavy ions in the moderate-energy range. We have compared this expression to the LSS theory and present suggestions that can be used as a basis for a more detailed approach to this problem.

The LSS theory, based on a Thomas-Fermi model of the interacting atoms, considers energy losses by electron stripping (ionization) and by nuclear collisions (nonionization) as uncorrelated and continuous processes. Recent publications⁴ present experimental results in terms of this theory in which the energy E in MeV and the range R in mg/cm² are reduced to dimensionless

* Work partially supported by the U.S. Atomic Energy Commission.

¹ N. Bohr, *Kgl. Danske Videnskab. Selskab, Mat.-Fys. Medd.* **18**, 8 (1948).

² J. Lindhard, M. Scharff, and H. E. Schiott, *Kgl. Danske Videnskab. Selskab, Mat.-Fys. Medd.* **33**, 14 (1963).

³ See, for example, (a) R. C. Axtmann and D. Kedem, *Nucl. Instr. Methods* **32**, 70 (1965); (b) C. B. Fulmer, *Phys. Rev.* **139**, B54 (1965); and (c) P. M. Mulas and R. C. Axtmann, *ibid.*, **146**, 296 (1966).

⁴ See, for example, (a) J. Gilat and J. M. Alexander, *Phys. Rev.* **136**, B1298 (1964); (b) N. K. Aras, M. P. Menon, and G. E. Gordon, *Nucl. Phys.* **69**, 337 (1965); (c) E. L. Haines and A. B. Whitehead, *Rev. Sci. Instr.* **37**, 190 (1966); (d) V. E. Noshkin, Jr., and T. T. Sugihara, *J. Inorg. Nucl. Chem.* **27**, 943 (1965). This last paper summarizes the previous empirical range-energy equations.

parameters ϵ and ρ , respectively, by the following equations:

$$\epsilon = [aM_2/Z_1Z_2e^2(M_1+M_2)]E, \quad (1)$$

$$\rho = [4\pi a^2 N_0 M_1 / (M_1+M_2)^2]R, \quad (2)$$

where $a=0.8853 a_0/(Z_1^{2/3}+Z_2^{2/3})$ and a_0 is the first Bohr radius, N_0 is Avogadro's number in terms of milligrams, e is the electronic charge, M is the atomic mass, Z is the nuclear charge, and the subscripts 1 and 2 refer to the incident and stopping media, respectively. For fission fragments, $Z_1=Z_p$, the most probable nuclear charge associated with the fragment mass. LSS have assumed that the electronic stopping expressed in ρ - ϵ units is $(d\epsilon/d\rho)e=ke^{1/2}$, where

$$k = \frac{0.0793\xi Z_1^{1/2}Z_2^{1/2}(M_1+M_2)^{3/2}}{(Z_1^{2/3}+Z_2^{2/3})^{3/4}M_1^{3/2}M_2^{1/2}}, \quad \xi = Z_1^{1/6}. \quad (3)$$

This assumption is discussed further in Sec. IV.B.

Integration of the electronic stopping gives the range in terms of $k\rho$ as a function of energy in terms of ϵ . In place of the cumbersome terms in Eqs. (1)–(3) we define the conversion constants specific for each ion-absorber combination as $A=\epsilon/E$ and $K=k\rho/R$. We use the latter to define a dimensionless absorber thickness τ as $\tau=KT$ with T in mg/cm^2 .

II. EXPERIMENTAL PROCEDURE

The basic equipment used for the experiments has been described previously.⁵ ORTEC silicon surface-barrier detectors, Model SBQN450–60 with resistivities of 650 and 875 $\Omega\text{-cm}$ were used with the reverse bias at 100 V. The fissile sources were U^{235} vapor deposited as 40 $\mu\text{g}/\text{cm}^2$ UO_2 ⁶ and approximately 3 μCi Cf^{252} prepared by the University of California Radiation Laboratory. The sources were 1.27 cm in diameter centered on 20-mg/ cm^2 stainless-steel substrates 1.52 cm in diameter. The Al, Ag, and Au absorbers were prepared by Seir Bath, Inc., the nickel absorbers were from Chromium Corporation of America, and the 20-wt%, 93% enriched U-Pd alloy absorbers were obtained from Brookhaven National Laboratory. The absorbers were mounted on 2.54-cm-i.d. rings and positioned approximately on the midplane between the source and detector which were 5.42 cm apart.

Each experiment consisted of measuring the degraded fission-fragment energy spectra through as many as 24 different absorber thicknesses with each source. Unattenuated spectra were taken for both sources immediately before and after each experiment. The precision mercury pulser was calibrated using the natural α 's from U^{233} , Am^{241} , and Cf^{252} sources at the start of each experiment. The calibration was checked

during and after each experiment and pulser check points taken after every third absorber spectrum. These checks allowed corrections to be made for the instrument drift caused by operating in an uncontrolled temperature environment. The drift rarely exceeded 3% over a 16-h period.

A. Absorber Thicknesses

The thickness of each absorber was determined by measuring the degraded energy of Cf^{252} α particles and using the α range-energy equations of Barkas and Berger.⁷ These equations are accurate to better than $\pm 1\%$. Gravimetric determination of the heavier foils agreed, in general, within 3% of the α energy measurements. The thicknesses given in Tables II–VI in Sec. III were calculated by the α degradation method.

B. Transmitted Energies

The apparent energies of the median-light and median-heavy fragments were calculated as the $\frac{1}{4}$ and $\frac{3}{4}$ quartile points for each integrated spectrum using the α calibrated pulser data to convert channel number to energy. These apparent energies were corrected for the charge collection losses, nonionization losses in the silicon, and losses through the gold window by the method we have described elsewhere^{8b} to obtain the true energies transmitted through the absorbers. It should be pointed out that the range-energy approximation that we used to correct for the window loss differed in form from the equation we present in Sec. IV. However, the difference in the results using the two equations is less than 0.1 MeV since the window thickness was approximately 40 $\mu\text{g}/\text{cm}^2$ (200 μ).

Table I gives the values for M_1 , the post-neutron emission mass; E_t^0 , the post-neutron emission unattenuated energy; and Z_p , the most probable nuclear charge for each median fragment type. The values for M_1 and E_t^0 were calculated from the data of Schmitt *et al.*⁸; those for Z_p were calculated by the equal-charge-displacement function using the data given by Glendenin and Unik.⁹

III. RESULTS

Tables II–V give the values of the energy E_t (MeV) transmitted by the absorbers of thickness T (mg/cm^2) for the median-light and median-heavy U^{235} and Cf^{252} fragments through Al, Ni, Ag, and Au. Table VI gives the data for Cf^{252} fragments through U-Pd. Table VII gives the values for A and K used to convert the experimental data to ϵ and τ for each fragment-absorber combination.

The individual plots of the energy-versus-thickness

⁵ (a) S. Kahn, R. Harman, and V. Fergue, *Nucl. Sci. Eng.* **23**, 8 (1965); and (b) V. Fergue and S. Kahn, *Nucl. Instr. Methods* (to be published).

⁶ R. Baciarelli, *Nucl. Appl.* **2**, 471 (1966).

⁷ W. H. Barkas and M. J. Berger, *Natl. Acad. Sci.—Natl. Res. Council Publ.* **1133**, 103 (1964).

⁸ H. W. Schmitt, J. H. Neiler, and F. J. Walter, *Phys. Rev.* **141**, 1146 (1966); and H. W. Schmitt (private communication).

⁹ L. Glendenin and J. Unik, *Phys. Rev.* **140**, B1301 (1965).

TABLE I. Post-neutron emission mass M_1 , energy E_t^0 and most probable nuclear charge Z_p for U^{235} and Cf^{252} fragments.

Source	Fragment	M_1 (amu)	Z_p	E_t^0 (MeV)
U^{235}	Light	95.34	38.60	100.13
	Average	116.74	46.00	84.89
	Heavy	138.14	53.40	69.63
Cf^{252}	Light	106.44	42.55	104.06
	Average	124.08	49.00	91.67
	Heavy	141.72	55.45	79.25

data in terms of ϵ and τ for each of the 18 fragment absorber combinations indicated that all of the curves had the same general shape but were displaced from each other by discrete increments of τ , $\Delta\tau$. A composite curve for each of the four fragment types in each absorber was obtained by shifting the τ axis by the quantity $\Delta_1\tau$ such that the ϵ_t^0 point fell on the best (by eye) curve through the points for the U^{235} light fragments. (For the U-Pd, this normalization was done relative to the Cf^{252} light fragments.) The five composite curves are shown in Fig. 1. Each curve in Fig. 1 is reproduced in Fig. 2 normalized by an additional increment $\Delta_2\tau$ such that each U^{235} light fragment ϵ_t^0 point fell on the Al curve. These $\Delta_2\tau$ points are shown as open circles in the figure. The data for the Al, Au, and U-Pd form a continuum over the region $12 \leq \epsilon \leq 348$; the curve for the nickel lies slightly above this, that for the silver lies slightly below it. The lower limit, $\epsilon=12$, corresponds to an apparent energy of approximately 10 MeV below which we were unable to obtain accurate

TABLE II. U^{235} and Cf^{252} median-light- and -heavy-fragment energies transmitted through Al absorbers.

T (mg/cm ²)	U^{235}		Cf^{252}	
	E_t (MeV) Light	E_t (MeV) Heavy	T (mg/cm ²)	E_t (MeV) Light Heavy
0.000	100.1	69.6	0.000	104.1 79.3
0.086	96.5	65.9	0.129	98.6 73.8
0.203	92.5	62.1	0.256	93.7 69.4
0.204	92.6	62.0	0.333	90.3 66.1
0.290	89.1	58.7	0.471	85.7 61.8
0.408	85.2	55.1	0.494	83.7 59.9
0.460	83.4	52.8	0.609	79.9 56.4
0.641	77.2	47.6	0.687	76.6 53.5
0.777	71.8	42.8	1.010	66.1 44.2
0.908	68.2	39.5	1.023	63.8 42.3
1.033	63.4	35.3	1.267	56.1 35.7
1.185	58.5	31.4	1.470	49.5 30.4
1.330	53.8	27.3	1.645	43.5 25.4
1.440	50.4	24.6	1.800	39.1 21.9
1.584	45.7	21.3	2.022	33.3 17.8
1.685	43.3	19.6	2.214	28.2 14.3
1.851	38.0	16.0	2.371	24.6
2.044	32.9	13.2	2.633	19.0
2.138	30.5		2.730	16.5
2.250	28.0		2.920	13.1
2.366	24.3			
2.452	22.2			
2.622	18.9			
2.889	13.6			

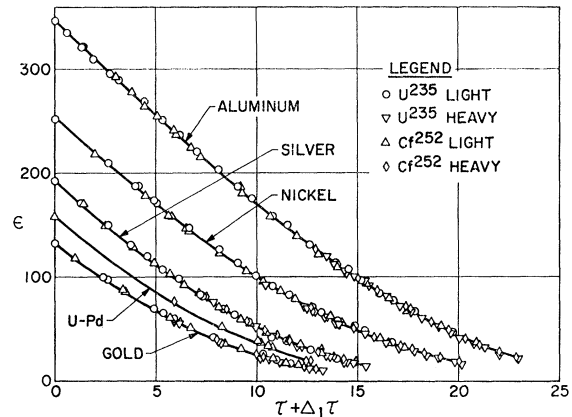


FIG. 1. Composite ϵ versus τ for each absorber.

measurements because of the reactor background in the U^{235} runs and the α pileup in the Cf^{252} runs.

The graphical extrapolation of the Al, Au, and U-Pd curve to $\epsilon=0$ in Fig. 2 gave an approximate value for the unattenuated range of U^{235} light fragments in Al, i.e., $k\rho^0=28.9$. This value was used as a starting point in an iterative curve-fitting procedure to obtain analytical values of $\Delta_1\tau$ and $\Delta_2\tau$. These values were then used to calculate a new value for $k\rho^0$ which was used as a new starting point. At the third iteration, $k\rho^0$ converged at 28.44; the equation relating range in energy, based on this value, was

$$k\rho = 1.158\epsilon^{1/2}[1 - \exp(-0.0987\epsilon)] + 0.01939\epsilon. \quad (4)$$

This equation was applied to the energy data for each fragment type through each absorber to calculate the residual range of the transmitted fragments. The total range was calculated for each datum point from

$$k\rho^0 = k\rho + \tau, \quad (5)$$

where τ is the dimensionless absorber thickness. Table

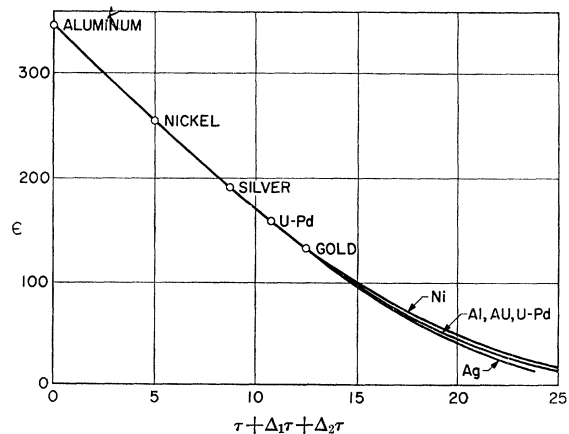


FIG. 2. Composite ϵ versus τ for all absorbers.

TABLE III. U²³⁵ and Cf²⁵² median-light- and -heavy-fragment energies transmitted through Ni absorbers.

T (mg/cm ²)	U ²³⁵ E _t (MeV)		Cf ²⁵² E _t (MeV)	
	Light	Heavy	Light	Heavy
0.000	100.1	69.6	104.1	79.3
0.625	83.0	53.8	85.2	61.7
0.628	82.9	53.6	85.2	61.6
0.934	73.9	46.1	76.1	53.7
0.965	73.9	46.2	75.2	52.9
1.154	68.5	41.9	70.3	48.8
1.184	67.6	41.2	69.2	47.9
1.559	58.1	34.0	59.1	39.8
1.899	49.7	28.1	50.8	33.6
2.118	44.9	24.9	45.8	29.7
2.338	40.3	21.8	41.3	26.4
2.524	36.1	19.0	37.3	23.6
2.713	32.6	16.8	33.9	21.1
2.963	28.3	14.2	29.5	18.2
3.083	26.1	13.0	27.2	16.4
3.272	23.3		24.2	14.5
3.591	18.6		19.7	
3.708	16.9		17.8	
3.900	14.6		15.6	

VIII gives the average values and the standard deviations for these ranges calculated by this method.

IV. DISCUSSION

Figure 3 compares Eq. (4) with range-energy data given in the literature¹⁰⁻¹⁴ for $\epsilon > 10$. The post-neutron emission energies associated with the individual fission-fragment masses and ranges given by Harvey¹⁰ were taken from Schmitt *et al.*⁸ as were the data for the factors A and K to convert to ϵ and $k\rho$ units. The values

TABLE IV. U²³⁵ and Cf²⁵² median-light- and -heavy-fragment energies transmitted through Ag absorbers.

T (mg/cm ²)	U ²³⁵ E _t (MeV)		Cf ²⁵² E _t (MeV)	
	Light	Heavy	Light	Heavy
0.000	100.1	69.6	104.1	79.3
0.494	88.8	58.3	91.9	67.3
1.005	77.5	48.0	79.6	55.7
1.429	68.5	40.4	69.7	47.1
1.732	62.3	35.6	63.3	41.7
2.025	56.1	31.0	56.7	36.5
2.320	50.8	27.4	51.5	32.5
2.737	43.3	22.4	43.5	26.6
2.814	42.0	21.8	42.5	26.0
3.161	35.5	17.1	36.3	21.5
3.360	33.1	15.9	33.5	19.5
3.655	29.9	14.1	29.1	16.5
4.096	21.8		24.0	
4.345	19.8		21.2	
4.788	15.5		16.6	
5.282	11.1		12.2	

¹⁰ B. G. Harvey, Ann. Rev. Nucl. Sci. 10, 235 (1960).

¹¹ L. Winsberg and J. M. Alexander, Phys. Rev. 121, 518 (1961).

¹² A. M. Poskanzer, Phys. Rev. 129, 385 (1963).

¹³ J. A. Davies, F. Brown, and M. McCargo, Can. J. Phys. 41, 829 (1963).

¹⁴ M. McCargo, F. Brown, and J. A. Davies, Can. J. Chem. 41, 2309 (1963).

TABLE V. U²³⁵ and Cf²⁵² median-light- and -heavy-fragment energies transmitted through Au absorbers.

T (mg/cm ²)	U ²³⁵ E _t (MeV)		Cf ²⁵² E _t (MeV)	
	Light	Heavy	Light	Heavy
0.000	100.1	69.6	104.1	79.3
1.636	75.6	46.7	77.9	54.7
1.756	74.4	45.6	75.5	52.7
3.316	53.1	29.6	53.3	34.9
3.645	49.5	27.1	49.4	32.0
4.012	45.4	24.5	45.3	29.1
5.260	31.7	15.9	32.0	19.7
5.768	27.0	13.2	27.2	16.4
6.940	18.1		18.0	
7.354	15.3		15.6	
7.803	12.7		13.1	

for Z_p were taken from Glendenin and Unik.⁹ Considering the different methods used to determine the ranges, i.e., the different definitions of what is meant by "range," the agreement between Eq. (4) and the literature data is remarkably good. Although there is no theoretical basis for this equation, this general agreement of other data to it can be taken as support for its empirical use, especially in the region above $\epsilon = 10$.

B. Comparison with LSS Theory

In their treatment of heavy-ion ranges, LSS² assume that the electronic stopping is given by

$$(d\epsilon/d\rho)_e = k\epsilon^{1/2}. \quad (6)$$

The nuclear stopping for $\epsilon^{1/2} \leq 4$ is derived from the Thomas-Fermi atom and is given by a curve [Fig. (2) of Ref. 2]. For $\epsilon^{1/2} \geq 6$, Rutherford scattering is effective and

$$(d\epsilon/d\rho)_n = (1/2\epsilon) \ln 2\epsilon. \quad (7)$$

For $4 < \epsilon^{1/2} < 6$, $(d\epsilon/d\rho)_n$ can be interpolated from the smooth joining of the LSS curve and Eq. (7). The total stopping, then, is given by

$$(d\epsilon/d\rho) = (d\epsilon/d\rho)_e + (d\epsilon/d\rho)_n \quad (8)$$

and the net range is the reciprocal of the integral of Eq. (8).

In order to simplify the results and the application of their theory, LSS calculated the net range for values of $k = 0.1, 0.2, 0.4$, and 1.6 as well as the electron strip-

TABLE VI. Cf²⁵² median-light- and -heavy-fragment energies transmitted through 20-wt% U-Pd, 93% enriched, absorbers.

T (mg/cm ²)	E _t (MeV)	
	Light	Heavy
0.00	104.1	79.2
3.69	34.1	19.8
3.75	34.2	20.2
4.48	25.7	
4.54	24.6	
4.70	21.2	
4.81	21.1	

TABLE VII. Values of the conversion factors A and K for U^{235} and Cf^{252} fission fragments in Al, Ni, Ag, Au, and 93% enriched, 20-wt% U-Pd alloy.

Source	Fragment	Al		Ni		Ag		Au		U-Pd ^a	
		A	K	A	K	A	K	A	K	A_c	K_c
U^{235}	Light	3.473	6.837	2.525	4.293	1.925	2.658	1.316	1.500		
	Average	2.383	5.568	1.800	3.639	1.421	2.327	1.005	1.357		
	Heavy	1.725	4.662	1.341	3.145	1.090	2.066	0.7939	1.238		
Cf^{252}	Light	2.825	6.119	2.098	3.929	1.631	2.476	1.136	1.423	1.529	2.243
	Average	2.097	5.217	1.602	3.454	1.278	2.233	0.9143	1.316	1.208	2.030
	Heavy	1.611	4.523	1.259	3.072	1.028	2.030	0.7523	1.226	0.9707	1.849

^a Calculated from $A_c = \sum f_i A_i$ and $K_c = \sum f_i K_i$, where A_i and K_i are the values of A and K for the i th component and f_i is the weight fraction of that component in the absorber.

ping range for these values of k . They then calculated an "effective" nuclear collision range $\Delta(k, \epsilon)$ as the difference between the electronic and net ranges for each of the four values of k for $1 \leq \epsilon \leq 1000$. Thus, for a given system, the LSS equations reduce to

$$k\rho = 2\epsilon^{1/2} - k\Delta(k, \epsilon). \quad (9)$$

Figure 4 compares $k\rho$ calculated for the unattenuated fragments in the absorbers by Eq. (9) with Eq. (4). The disagreement in this figure is comparable to that given by LSS when they compared their theory to other experimental results in the same region of ϵ (Fig. 14 of Ref. 5).

Throughout the present data reduction and analysis, the values used for k in Eq. (4) were those calculated from Eq. (3). However, inspection of this equation indicates two potentially weak points, i.e., that $\xi = Z_p^{1/6}$ and that the electronic stopping power is directly proportional to the ion velocity. These two assumptions were briefly investigated using the following general derivation for the constant k' in

$$(d\epsilon/d\rho)_\epsilon = k'\epsilon^w. \quad (10)$$

The stopping power in ϵ - ρ units is

$$(d\epsilon/d\rho)_\epsilon = S_e [(M_1 + M_2) / 4\pi e^2 a Z_p Z_2 M_1] \quad (11)$$

with

$$S_e = \xi 8\pi e^2 a_0 (Z_p Z_2 / Z) (v/v_0)^{2w}, \quad (12)$$

$$v = 1.387 \times 10^9 (E^{1/2} / M_1^{1/2}), \quad (13)$$

$$E = [Z_p Z_2 e^2 (M_1 + M_2) / a M_2] \epsilon, \quad (14)$$

where $e^2 = 2.309 \times 10^{-10}$ erg cm, a_0 is the first Bohr radius = 5.292×10^{-9} cm, $a = 0.8856 a_0 / Z^{1/3}$, $Z = (Z_p^{2/3} + Z_2^{2/3})^{3/2}$, v_0 is the velocity of first Bohr electron = 2.182×10^8 cm/sec, v is the ion velocity (cm/sec), and E is the ion energy (MeV). Combining Eqs. (11)–(14) and simplifying gives

$$\left(\frac{d\epsilon}{d\rho} \right)_\epsilon = \left[\frac{(2.259) (M_1 + M_2) \xi}{(Z_p^{2/3} + Z_2^{2/3}) M_1} \right] \left[\frac{0.001248 (Z_p^{2/3} + Z_2^{2/3})^{1/2} (M_1 + M_2) (Z_p Z_2)}{M_1 M_2} \right]^w \epsilon^w, \quad (15)$$

where k' is the product of two bracketed terms. When $w = 0.5$, this product reduces to Eq. (3), $k' = k$ and Eq. (15) is identical to Eq. (6).

A best fit for ξ was sought by setting $w = 0.5$ and varying k' in 0.01 increments from 0.1 to 0.3 in Eq. (15). Each value was used in the integration of Eq. (8) to obtain ρ as a function of ϵ . The interpolated results indicated that setting $\xi = Z_p^{0.206}$ gave better agreement with the data from Eq. (4) than did $\xi = Z_p^{1/6}$. This is remarkably close to the function $\xi = Z_p^{0.211}$ derived by Aras *et al.*^{4b} However, the detailed comparison still showed deviations similar to but less pronounced than those indicated in Fig. 4.

The procedure was repeated setting $\xi = Z_p^{1/6}$ and varying w in increments of 0.05 to 0.35 to 0.65. The results were converted to ϵ - τ units and compared to the experimental data in the same units. Although the general trend indicated that the best agreement could be obtained with $w = 0.55$, there were many deviations from this.

An attempt was made to investigate this further by varying both ξ and w . However, a brief analysis of the

TABLE VIII. Average range of median-light and -heavy U^{235} and Cf^{252} fission fragments in Al, Ni, Ag, Au, and 20-wt% U-Pd.

Absorber	Fragment	R (mg/cm ²)	% σ
Al	U-Light	4.17	0.325
	Heavy	3.22	0.365
	Cf-Light	4.16	0.364
	Heavy	3.44	0.396
Ni	U-Light	5.53	1.16
	Heavy	4.30	2.22
	Cf-Light	5.52	1.46
	Heavy	4.57	2.49
Ag	U-Light	7.33	1.01
	Heavy	5.50	0.950
	Cf-Light	7.28	0.820
	Heavy	5.82	0.948
Au	U-Light	10.66	0.496
	Heavy	7.81	0.351
	Cf-Light	10.47	0.343
	Heavy	8.27	0.402
U-Pd	Cf-Light	7.90	0.747
	Heavy	6.29	0.660

results indicated that there was no one general form that gave good agreement for all cases.

V. SUGGESTED THEORETICAL APPROACH

At present there are two theories that attempt to describe the stopping of fission fragments; the LSS theory and the earlier Bohr theory. Both theories consider the nuclear stopping and electronic stopping as separate mechanisms. Bohr assumed that the nuclear stopping could be completely expressed by Rutherford scattering while LSS took into account the Thomas-Fermi characteristics of atoms. This latter model gives the better agreement with published data^{4c,15,16} for heavy ions in the very low velocity region where nuclear collisions are the dominant mechanism and there is nothing in the present work to contradict this. The problem appears, then, to be primarily associated with the electronic stopping term. The Bohr equation gives this as a logarithmic function of velocity while the LSS equation assumes that it is a power function of velocity.

There are two parameters in the Bohr formulation which are not easily evaluated from first principles and thus are the most likely sources of errors of approximation. It should be noted that the same parameters must be considered in the derivation of the LSS cross section [Eq. (12)] but the exact nature of the approximation they used has not been published as yet.¹⁷ Therefore, in the following, these parameters will be discussed only in terms of the Bohr theory.

The first parameter of interest is Z_{eff} , the ionic charge of the fragment, the square of which appears in the equation for the cross section. This must be a function of the fragment velocity, i.e., it must decrease from

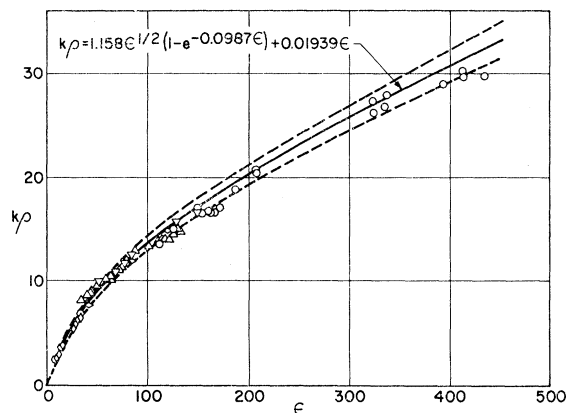


FIG. 3. Comparison of Eq. (4), derived empirically in this work, with literature range-energy data for $10 \leq \epsilon \leq 450$. Open triangles U^{235} in U, Ref. 10; open circles: U^{235} in Al, Ref. 10; open squares. U^{235} in Au, Ref. 10; solid triangle: Ar^{41} in Al, Ref. 13; solid circles: Tb^{149} in Al, Ref. 11; solid squares: Ne^{22} in Al, Ref. 12. Dashed lines represent $\pm 5\%$ envelope around equation (4).

¹⁵ P. G. Bizzeti, A. M. Bizzeti-Sona, G. Dicaporiaco, and M. Mando, Nucl. Instr. Methods **34**, 261 (1965).

¹⁶ A. R. Sattler, Phys. Rev. **138**, A1815 (1965).

¹⁷ J. Lindhard and M. Scharff (unpublished).

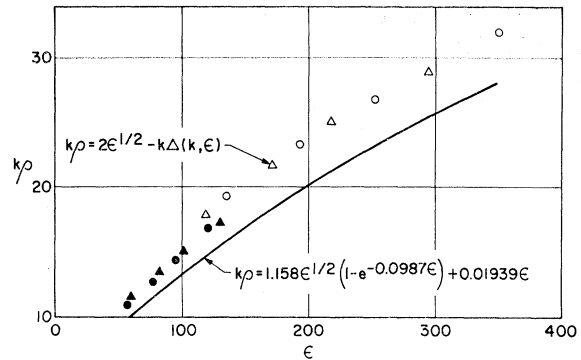


FIG. 4. Comparison of LSS theoretical total ranges (points) with experimental total ranges (line). Open circles: U^{235} light fragments; solid circles: U^{235} heavy fragments; open triangles: Cf^{252} light fragments; solid triangles: Cf^{252} heavy fragments. Pairs of points in each set (open and solid) represent the data, from left to right, for gold, silver, nickel, and aluminum.

about 20 at the virginal velocity to 0-1 in the region of $v_0 = e^2/h$. The exact dependence of Z_{eff} on velocity is not given simply from first principles and approximations are rather sensitive to the atomic model used. Various authors^{1,2,18-20} have given simple relationships based on assumptions regarding the binding of the outermost electrons on the fragment; none of these relationships fit the experimental data.²¹

A more difficult approach suggested by Bell²² involved examination of the probabilities of capture or loss of an electron by the fragment in collision with individual atoms of the stopping medium. Again, the results are sensitive to the atomic model adopted and the way the collision is treated. Bell's calculations did not agree closely with the data for the limited cases calculated, but a modification of the technique by Gluckstein²³ succeeded in matching data²⁴ on oxygen and neon ions rather well. The modification, if applied to Bell's original calculations, would considerably improve the agreement for fission fragments. In addition, Bohr and Lindhard²⁵ adopted a similar technique with slight changes in assumptions and produced fair agreement with Lassen's²¹ data.

This approach has certain additional benefits. The pressure-density effects associated with gaseous stopping media as well as the difference between solid and gaseous materials can be treated with relative ease. It is also possible that within the limits of quantum-mechanical restrictions, the energy distribution of the secondary electrons may be obtainable. This has im-

¹⁸ W. E. Lamb, Jr., Phys. Rev. **58**, 696 (1940).

¹⁹ J. K. Knipp and E. Teller, Phys. Rev. **59**, 659 (1940).

²⁰ J. H. M. Brunnings, J. K. Knipp, and E. Teller, Phys. Rev. **60**, 657 (1941).

²¹ N. O. Lassen, Ph.D. thesis, Copenhagen, 1952 (unpublished).

²² G. I. Bell, Phys. Rev. **90**, 548 (1953).

²³ R. L. Gluckstein, Phys. Rev. **98**, 1817 (1955).

²⁴ E. L. Hubbard and E. J. Laver, Phys. Rev. **99**, 1914 (1955).

²⁵ N. Bohr and J. Lindhard, Kgl. Danske Videnskab. Selskab. Mat.-Fys. Medd. **28**, 7 (1954).

plications both for radiation chemistry and for a rigorous determination of the charge collection loss in the pulse-height defect.^{5b}

In general, Bell's approach offers good possibilities for solving one of the prime theoretical problems in the physics of fission-fragment energy loss and should shed light on some more practical problems. The drawbacks are the extreme complexity of the calculations for any given case (reflected by the paucity of cases for which actual calculations have been carried out) and the possible requirement for parametric adjustment in the models used. Both of these problems should be greatly mitigated by the availability of high-speed digital computers.

A simpler empirical technique was used recently by Dmitriev²⁶ to determine Z_{eff} as a function of velocity for ions up to argon. It is possible that extrapolation of this function to fission fragments may produce sufficient accuracy but the calculations have not been carried out. Along the same line, Nikolaev²⁷ has calculated capture and loss cross sections which should provide good checks of the Bell-type calculations at some points.

Another of the major theoretical problems arises in the "stopping number,"

$$B = Z_2 \ln \frac{1.123mv^3h}{Ie^2Z_{\text{eff}}}. \quad (16)$$

The difficulty is that because of shell effects, the value of the average excitation potential I for an electron of the stopping medium, which must be experimentally determined, is not truly independent of the velocity. It is usually determined using high-energy protons for which the velocity dependence is negligible. For particles of lower velocities, correction terms C_i for the velocity effect due to the i th shell are introduced into B in Eq. (16). Livingston and Bethe²⁸ give velocity-dependent formulae for C_K (K shell); Hirschfelder and

Magee²⁹ have extended the technique to approximate the correction terms for the outer shells in the case of low-velocity protons. Their approach might prove applicable to the relatively low velocities of fission fragments.

Another approach, using our experimental data, can be suggested. If Eq. (16) is rewritten as

$$B = Z_2 \ln \frac{1.123mv^3h}{e^2Z_{\text{eff}}} - \sum \eta_i \ln I_i, \quad (17)$$

where η_i is the oscillator strength of shell i ($\sum \eta_i = Z_2$), and I_i is the excitation potential of shell i , and given values of B from the data are substituted for each of the fragment types at a given velocity in a given material, values of I_i can be calculated. Values of η_i for shells above the L shell are uncertain, but reasonable first approximations plus the use of iteration techniques to produce smooth fits of the I_i versus v and Z_2 over the wide range of data should give the desired results. The atomic model which produces the best results for Z_{eff} should also lend guidance in choosing the values of the η_i .

In summary, neither the theoretical systems as presently formulated nor our empirical fitting techniques have totally resolved the problem of fission-fragment interactions with matter. Combinations of the more microscopic and complex approaches briefly summarized here hold great promise for producing a general solution to this problem, especially when bolstered by recourse to the present experimental data for parametric adjustment. The complexity of the calculations over many variables for any one case, multiplied by the sheer volume of cases, places the task well beyond the scope of the present work; with proper use of high-speed computers the difficulties would not seem to be insurmountable.

ACKNOWLEDGMENTS

We wish to thank S. Shope and R. Harman for their technical assistance and J. Cusack and L. Carpenter for their valuable comments and criticisms.

²⁶ I. S. Dmitriev, Zh. Eksperim i Teor. Fiz. **47**, 615 (1964) [English transl.: Soviet Phys.—JETP **20**, 409 (1965)].

²⁷ V. S. Nikolaev, Usp. Fiz. Nauk **85**, 679 (1965) [English transl.: Soviet Phys.—Usp. **8**, 269 (1965)].

²⁸ M. Livingston and H. Bethe, Rev. Mod. Phys. **9**, 245 (1937).

²⁹ J. O. Hirschfelder and J. L. Magee, Phys. Rev. **73**, 207 (1948).